175 HP at .55

BSFC

Snce/Kurutn
613.5

SAE Technical Paper Series

820354

Preliminary Results on Performance Testing of a Turbocharged Rotary Combustion Engine

P. R. Meng,
W. J. Rice,
H. J. Schock, and
D. P. Pringle
NASA Lewis Research Center
Cleveland, OH

Preliminary Results on Performance Testing of a Turbocharged Rotary Combustion Engine

P. R. Meng, W. J. Rice, H. J. Schock, and D. P. Pringle

NASA Lewis Research Center
Cleveland, OH

THE ROTARY COMBUSTION ENGINE (RCE) is of interest as a future powerplant for general aviation (g/a) and other small aircraft because of its turbine-like characteristics of simplicity, compactness, high specific power, improved fuel tolerance, low vibration and noise levels and clean, low drag installation characteristics. It is uniquely adaptable to stratified-charge, multifuel operation, with which it gives reasonable brake specific fuel consumption (BSFC) and exhaust emission levels. This will help solve the fuels cost/availability problem, which is generally considered the most important single issue facing general aviation today. An advanced rotary was selected in several recent mission studies (1, 2, 3)* as being the most promising among several alternative candidate light aircraft engines for the future.

In the interest of evaluating the rotary engine for g/a, NASA contracted with Curtiss-Wright Corporation to test an existing naturally aspirated rotary aircraft engine. The test data on this carbureted 285 HP (212 Kw), gasoline rotary aircraft engine showed that the BSFC and HC emissions were slightly high (4). BSFC at cruise conditions (77 percent power) was 0.54 lb/BHP-hr (328 g/Kw-hr), about 20 percent higher than the best current aircraft piston engines of comparable power. However, the engine specific weight was 1.26

*Parenthetical numbers indicate references listed at end of this paper.

lb/HP (0.766 Kq/Kw) which is at least 15 percent lower than today's best aircraft engines. A follow-on contract (5) which incorporated several slight modifications to this engine reduced the cruise BSFC to 0.45 lb/BHP-hr (274 g/Kw-hr) while meeting the formerly proposed aircraft emission standards. Further advances in rotary engine technology have been made by Curtiss-Wright Corporation in the design and development of a 1500 HP (1119 Kw) stratified charge engine under a contract with the United States Marine Corps. This four rotor multifuel engine was successfully tested and has achieved the required design goals (6). This engine design was used as a baseline for further NASA rotary engine conceptual design studies (7, 8). The results of the Advanced Stratified-Charge Rotary Aircraft Engine Conceptual Design Study have indicated that a highly advanced stratified-charge aircraft engine could achieve cruise BSFC's of 0.36 lb/BHP-hr (219 g/Kw-hr) at 250 BHP (186.4 Kw) with a specific weight of 0.80 lb/BHP (0.486 Kg/Kw). The major specific weight improvement occurs from turbocharging a stratified charge, multifuel rotary engine (7). Turbocompounding can make further improvements in BSFC or specific weight for larger engines as discussed in Reference (8). At this time there are no experimental data available on the performance of turbocharged rotary engines. The preliminary test results obtained by turbocharging a Mazda non-emis-

---

ABSTRACT

The purpose of these experiments was to determine the performance of a turbocharged rotary engine at power levels above 75 kw (100 hp). A twin rotor turbocharged Mazda engine was tested at speeds of 3000 to 6000 rpm and boost pressures to 7 psi.

The NASA-developed combustion diagnostic instrumentation was used to quantify IMEP, PMEP, peak pressure and face-to-face variability on a cycle-by-cycle basis.

Results of this testing showed that at 5900 RPM a 36 percent increase in power was obtained by operating the engine in the turbocharged configuration. When operating with lean carburetor jets at 105 hp (78.3 kw) and 4000 RPM, a brake specific fuel consumption of 0.45 lbm/lb-hr was measured.

sions controlled, carbureted automotive engine with a commercially available turbocharger are presented in this report.

FACILITY AND INSTRUMENTATION

DESCRIPTION OF FACILITY - The test program was conducted at NASA Lewis Research Center. Figure 1 is a photograph of the rotary engine and turbocharger system tested. A description of this engine is given in Table 1.

A BAE commercial turbocharger kit (System No. 13-0000) was installed as specified in the manufacturer's instructions. Modifications were made to the inlet and exhaust systems to adapt them to the engine test facility. Boost pressure was maintained at a constant level over the range of engine speed by supplying pressurized air to the diaphragm of the waste gate. The wastegate is shown to the left of the turbine and just below the exhaust pipe in Figure 1. A four speed manual transmission was utilized to couple the engine to a 250 HP (186.4 Kw) dynamometer. This dynamometer is limited to a maximum speed of 6000 RPM. This limitation prevented testing of the engine at its naturally aspirated rated speed of 7000 RPM without shifting the transmission to a lower gear. Tests were conducted in fourth gear (direct-drive) to eliminate changes in

Fig. 1 - Rotary engine with turbocharger system installed

Table 1

Mazda 12B Spark-Ignition Engine

Compression Ratio 9.4:1
Rating Naturally Aspirated 110 HP at 7000
Output Turbocharged 153 HP at 5900 RPM
Carburetted, 2 Rotor, 35 in^3/Rotor* 573 cc/rotor
Fuel: Clear Indolene
    RON 97.6, MON 87.6

* 35 in^3 = Maximum Volume - Minimum Volume for 1 Rotor Face

frictional characteristics of the transmission. Transmissions of this type have been shown to have efficiencies of 98 percent in direct-drive at high power levels (9); however, for the purposes of this paper a 100 percent transmission efficiency is assumed. This results in consistent but slightly pessimistic data.

Complete conventional pressure, temperature and flow instrumentation was installed on the engine in addition to the special NASA-developed combustion instrumentation which will be discussed later in this report. Automatic control systems were utilized for engine speed, dynamometer load, and coolant discharge temperature. Load was measured with a reaction load cell. An absolute position optical shaft angle encoder was installed on the front of the engine and was belt-driven at a 3:2 ratio by the eccentric shaft to provide rotor angle information. The 3:2 ratio was used to convert the 1080° crank degree cycle of the RCE to 720° so as to be analogous to the four stroke piston engine cycle.

Exhaust emissions were measured by a Scott Research Laboratories Test Console which incorporated the following equipment:

A Scott Model 415   Total HC Analyzer
A Scott Model 250   Paramagnetic O_2 Detector
A Scott Model 125   NO/NO_x Analyzer
A Beckman Model 864 CO_2 Analyzer
A Beckman Model 865   CO Analyzer

Engine operation was monitored on the alpha-numeric CRT displays in the control room. A micro-processor at the test cell was utilized to interface with a central minicomputer which performed on line calculations and continuously updated the CRT displays. An IBM-3033 was used for necessary post-run processing and graphical analysis of collected data.

SPECIAL INSTRUMENTATION - In addition to the standard instrumentation, unique NASA-developed combustion diagnostic instrumentation (10, 11) was used to obtain data on key
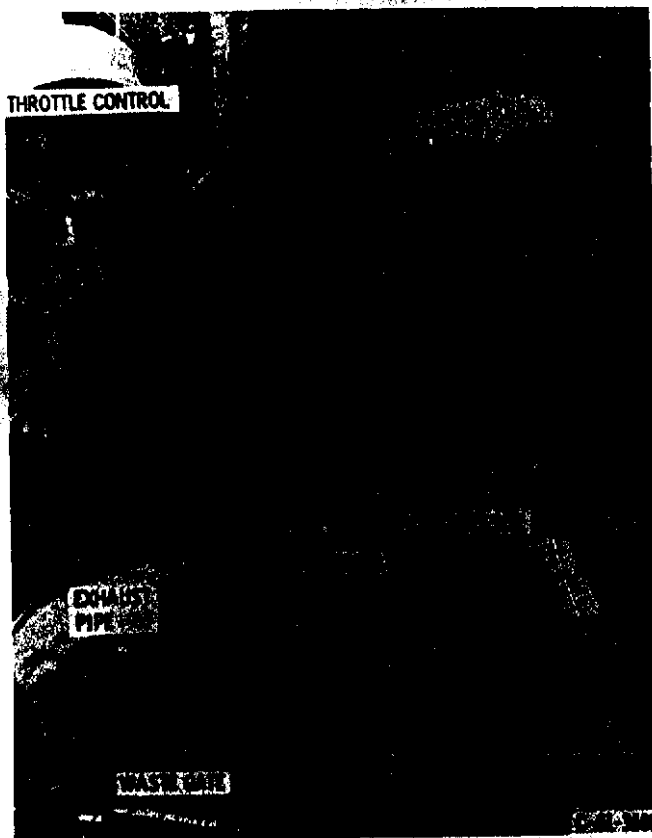
combustion parameters. Real time measurements were made of indicated mean effective pressure (IMEP), pumping mean effective pressure (PMEP), peak cycle pressure, angle of occurrence of peak pressure and the spark timing. This instrumentation system is capable of measuring these parameters on a cycle-by-cycle basis. It is also valuable in determining the effects of changes in global air-fuel ratio, combustion chamber shape, and spark advance on the combustion process. Data is presented in histogram form on an oscilloscope and computations of mean, standard deviation, maximum and minimum values are available as digital output. Figure 2 shows a typical histogram of IMEPT (IMEPT = IMEP + PMEP) for the engine tested. This diagnostic instrumentation as installed in the control room, is shown in the foreground of Figure 3.
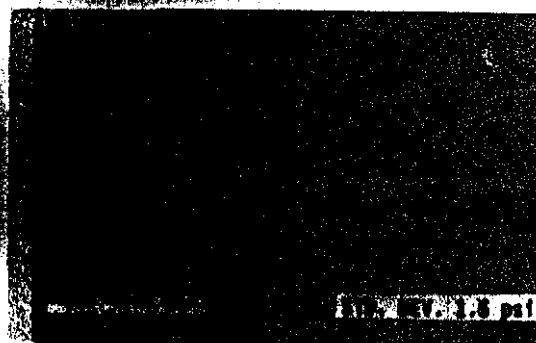
Pressure-volume diagrams are also generated by the diagnostic instrumentation. Figure 4a shows a typical diagram of the complete four stroke cycle and Figure 4b shows a blowup of the pumping loop of the diagram for a condition when the engine was in turbocharged operation at 4 psi (27.6 kpa) boost. The diagnostic equipment would also be useful for tuning the inlet and/or exhaust systems; however, no attempt was made to do this during this series of tests.
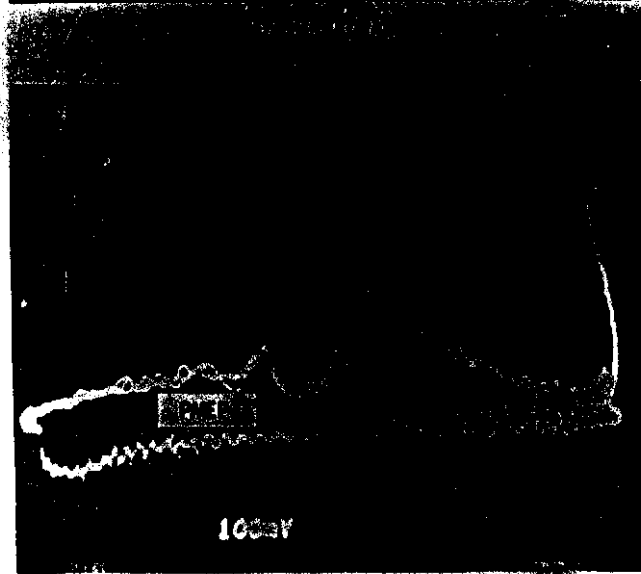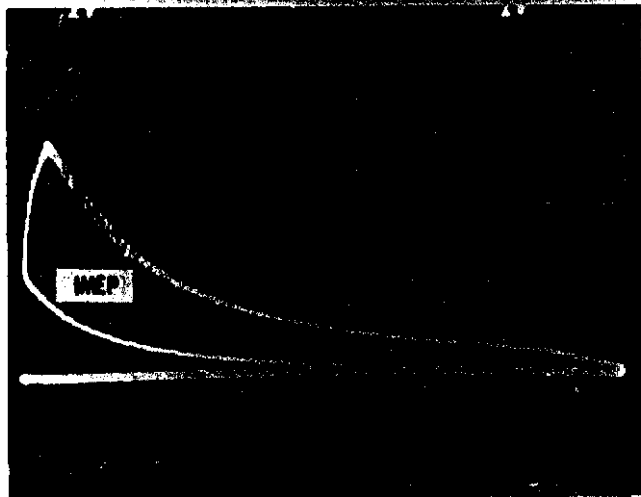
A new feature of this system was the ability to make measurements in any of the three combustion faces of the rotor by electronically switching to the face of interest without stopping the engine. This feature allowed measurements of IMEPT for the three rotor faces while the engine was at the same thermal equilibrium point. Figure 5 shows there is little face to face variation in IMEPT over the region tested. Each of the nine points on this graph represents the average of one hundred consecutive measurements of IMEPT. Maximum variability defined as (max-min)/average was 2.8 percent at 5000 RPM.

TEST PROCEDURE — The engine was operated at steady state conditions (speed, load and water temperature), at which time data were recorded and oscilloscope traces from the combustion instrumentation were photographed. Steady state was said to exist when there was agreement of ± 5 percent between the air/fuel (A/F) ratio from the direct measurement of air flow and fuel flow and the A/F ratio calculated from the method of Spindt (12).

After the engine was brought to the test speed, load and boost were applied until the desired boost was attained at a given load. Spark was advanced to the point of audible knock and then retarded slightly. (The trailing spark plug was fired 10 eccentric shaft degrees later than the leading plug.) Initial tests were conducted using water injection to control knock. This method was found to be very effective; however, the emis-

Fig. 2 — Typical bargraph of one hundred consecutive cycle values of IMEPT for rotary engine

CS-81-1017

Fig. 3 — Photograph of test cell control room

(b) PUMPING LOOP

Fig. 4 - P-V diagram and blowup of pumping loop at 4000 RPM, 4 psi (27.6 kpa) boost, and 105 BHP (78 kw)
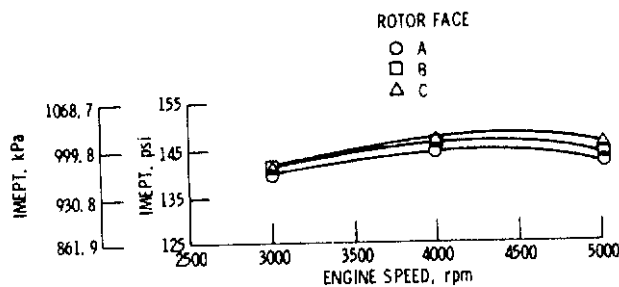
sion analyzer was adversely affected by the additional water from injection and the practice was discontinued. None of the test conditions for the data presented in this report include water injection.

EFFECT OF BOOST - The data in Figure 6 show the range of speeds and powers (BHP) over which the engine was tested. The upper curve shows the output of the turbocharged engine at boost pressures of up to 7 psi (48.3 kpa), and the lower curve shows the wide-open throttle performance of the engine naturally aspirated. A comparison of the performance of this engine in the turbocharged configuration with the naturally aspirated system shows a 36 percent increase in power from 112.5 BHP (83.9 Kw) to 153 BHP (114 Kw) at a nominal speed of 5900 RPM. Power levels at the three boost levels of 3, 5, and 7 psi (20.7, 34.5, and 48.3 kpa) over a range of speed from 3000 to 6000 RPM are shown in Figure 7.

COOLANT TEMPERATURE EFFECT ON BSFC - Researchers at General Motors (13) have shown that an increase in coolant temperature from $190°$ F to $280°$ F ($88°$ C to $138°$ C) resulted in reductions in hydrocarbon emissions by a factor of 3 in a rotary engine. Another recent publication (14) showed a significant improvement in BSFC as coolant temperature was increased from $140°$ F to $212°$ F ($60°$ C to $100°$ C). A reduction in HC emissions was also observed in this study. In both these instances, the tests were conducted over a range of speeds and loads necessary for road load operation of an automobile. It was our intention to determine whether or not the fuel economy at the higher speeds and power ranges of interest for aircraft application would also be affected by changes in housing coolant temperature. A thermocouple installed near the epitrochoidal surface of the rotor housing (Figure 8) was used to measure the surface temperature during testing.
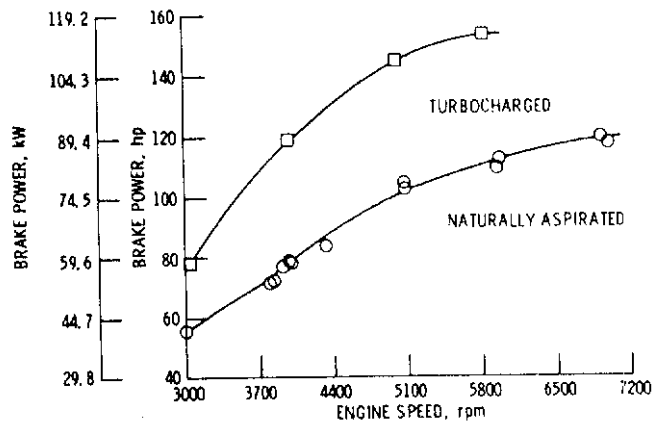

Fig. 5 - Variability of IMEPT on rotor faces

Fig. 6 - Power output of turbocharged and naturally aspirated rotary combustion engine as a function of speed

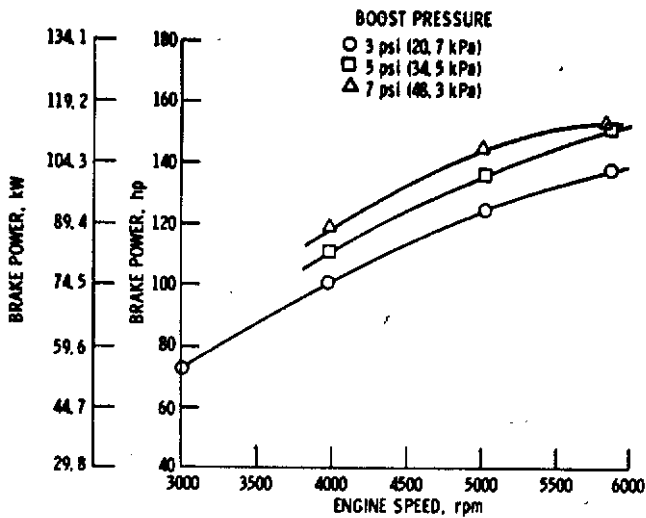Fig. 7 – Power output of rotary combustion engine at various levels of boost pressure
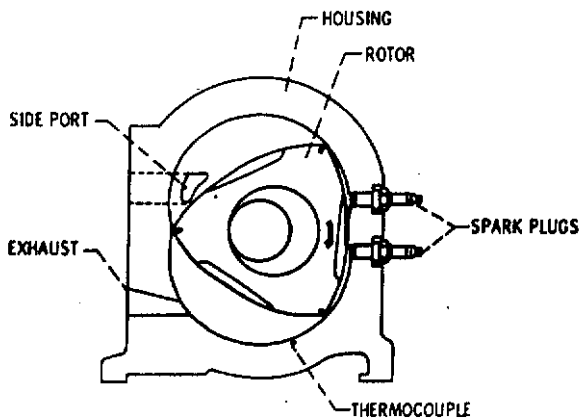

Fig. 9 – Coolant discharge temperature versus speed at a constant power of 105 BHP (78 kw)

Fig. 8 – Location of thermocouple on rotor housing surface
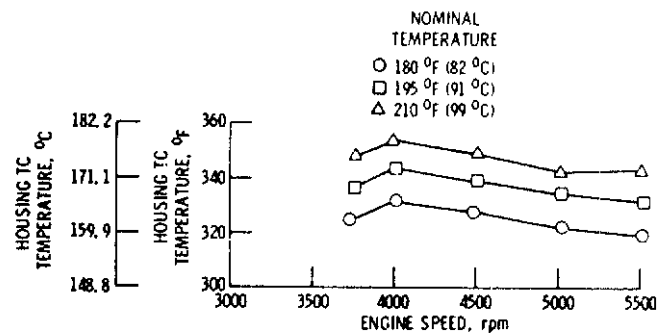
Fig. 10 – Variation in housing surface temperature with speed at three coolant discharge temperatures

Coolant discharge temperatures are shown in Figure 9 and corresponding housing thermocouple readings are shown in Figure 10. Conditions studied were at a constant power of 105 BHP (78.3 Kw) and speeds ranging from 3500 to 5900 RPM. Figure 11 shows that no discernible differences in fuel economy were found as the coolant discharge temperature changes from 180° F to 210° F (82° C to 99° C).

It is interesting to note in Figure 12 that at a given speed with increasing coolant temperature there appears to be a general reduction in hydrocarbons. The rich carburetor jets used in this testing were used to keep turbine inlet temperatures within tolerable limits. For each of the speeds, there was no recognizable change in A/F ratio which would have biased this comparison.
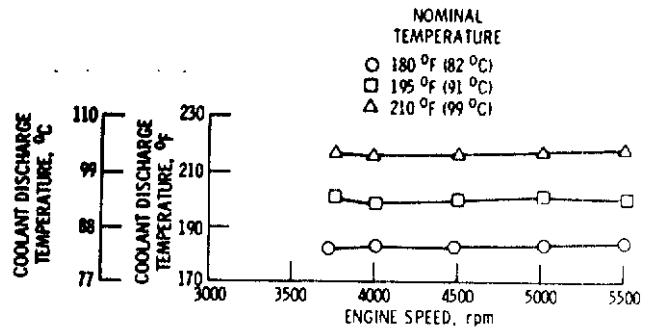

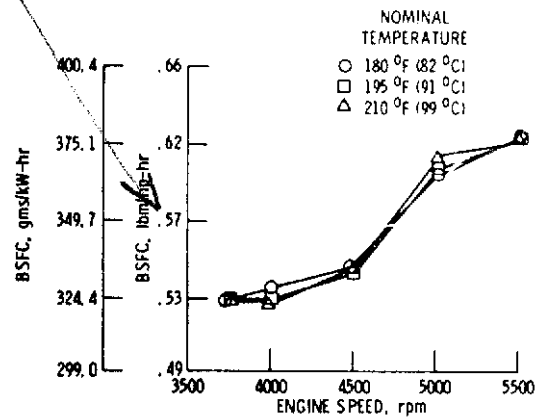Fig. 11 – Variation of BSFC with coolant discharge temperature at constant power of 105 BHP (78 kw)

EFFECT OF A/F RATIO ON BSFC AT CRUISE CONDITIONS (105 BHP) (78.3 Kw) – Smaller carburetor jets were installed to determine their effect on BSFC and turbine inlet temperature. Figure 13 shows the variation in A/F ratio for the two sets of carburetor jets. Coolant discharge temperature from the engine block was maintained at 180° F for all conditions. The lower curve is for the larger jets and the upper curve for the smaller jets. Figure 14 shows the corresponding BSFCs for these conditions. The most economical point on the lower curve is approximately 0.45 lbm/HP-hr (274 g/Kw-hr) compared to 0.54 (328 g/Kw-hr) at the same power and speed but lower A/F ratio. Clearly, one would prefer to operate at the leaner condition and realize the 16 percent improvement in fuel consumption. However, the normal continuous operation temperature limit of typical turbochargers is 1650° F (899° C), and examination of the data in Figure 15 shows that the temperature limit was exceeded by up to 200° F (111° C) while operating the engine at the lean conditions. This increase in turbine inlet temperature at lean operating conditions in combination with high stresses over an extended period of time may cause turbine failure.

The most desirable way to reduce the Exhaust Gas Temperature (EGT) is to devise a method of burning the fuel earlier in the expansion stroke. This means that more of the energy would be extracted from the air-fuel mixture as work. This action would have to take place within the structural limitations of the engine.

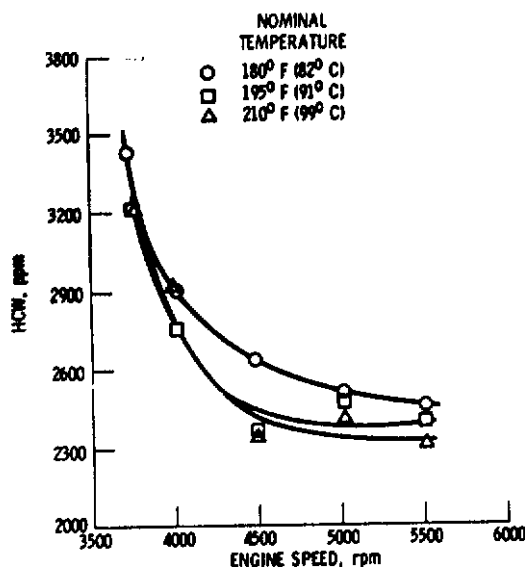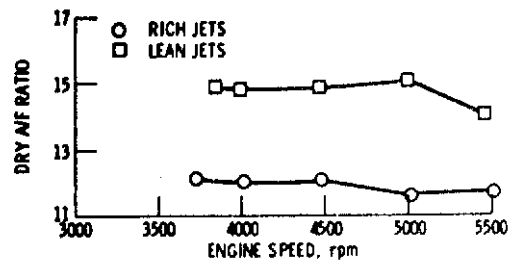**DIESEL VS. ROTARY ENGINE ENERGY USAGE** – Figure 16 gives an energy balance for the RC

Fig. 13 – Air-fuel ratio versus speed for rich and lean carburetor jets at a constant power of 105 BHP (78 kw)
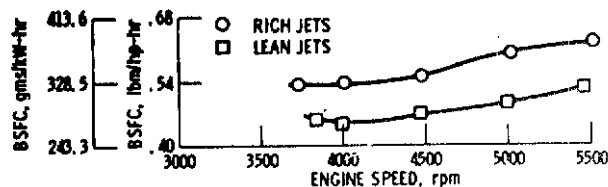

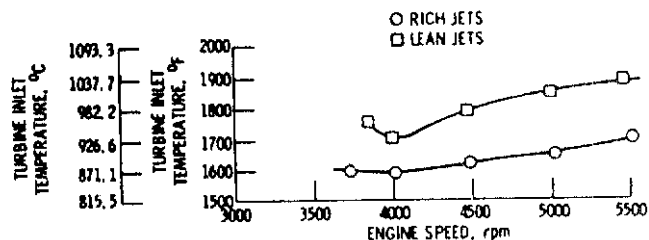Fig. 14 – BSFC versus speed for rich and lean carburetor jets at constant power of 105 BHP (78 kw)

Fig. 15 – Turbine inlet temperature versus speed for rich and lean carburetor jets at a constant power of 105 BHP (78 kw)

Fig. 12 – Variation of hydrocarbon emissions with coolant discharge temperature at constant power of 105 BHP (78 kw)

engine tested. This graph is for a constant power of 105 BHP (78.3 Kw) at 155 psi (1069 kpa) BMEP and 3990 RPM. The spark was advanced to MBT timing for this test condition. This figure shows how the energy input into the rotary combustion engine can be divided among useful work, heat rejection to exhaust, coolant and oil, and "miscellaneous." The latter term includes the previously-discussed transmission losses, as well amounts for convection, radiation and windage. Similar results are shown on Figure 17 for a turbocharged direct-injection AVL research diesel engine (description in Table 2). In a gross sense, these graphs give an indication of where research effort should
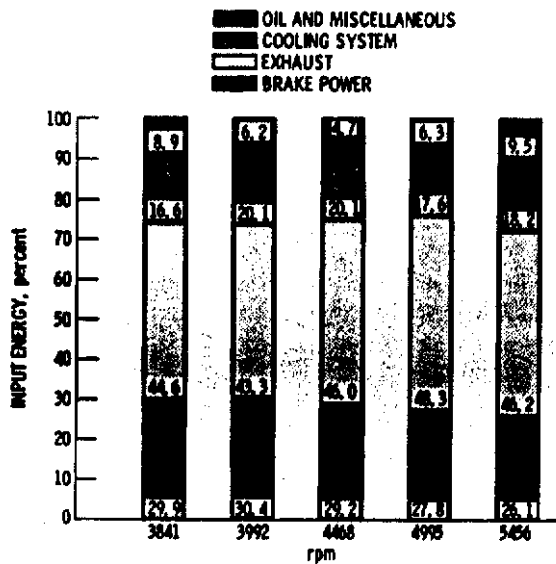
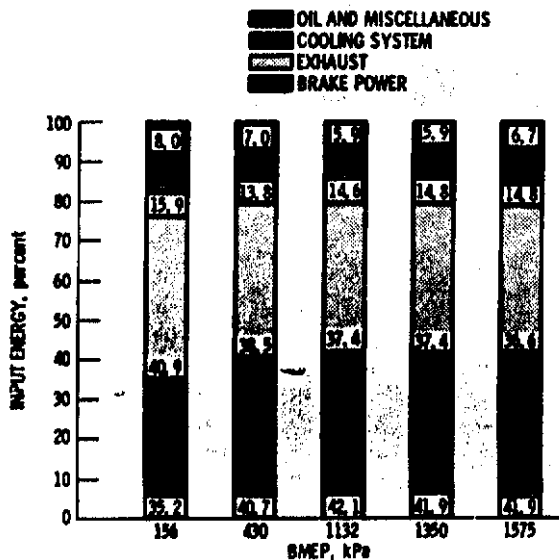Fig. 16 – Energy balance of turbocharged rotary combustion engine at constant power of 105 BHP (78 kw)

Fig. 17 – Energy balance of turbocharged diesel at constant speed of 1500 RPM

Table 2

AVL-521 Research Diesel Engine

Compression Ratio - 17.3/1
80 BHP at 3000 RPM Supercharged to 47.7 PSIA
Fuel Injected-Single Cylinder, 87.8 in³ Disp.
Fuel No. 2 Diesel

be expended. The rotary engine tested is compared to the diesel since one would like to approach the high efficiency of the diesel engine in the lightweight rotary for aircraft applications. However, it should be kept in mind that this heat balance comparison was made with a stratified charge combustion diesel engine and a homogeneously charged rotary combustion engine which will account for some of the differences in energy recovery. Some of the discussion which follows is admittedly speculative in nature but it does represent an attempt to describe the important aspects of combustion and efficiency of the diesel relative to the rotary engine.

The rotary engine shows an average brake energy recovery rate of 29 percent after the transmission while that for the diesel is 40 percent. The diesel operates at a much higher compression ratio, which with its injection controlled rate of heat release results in a more favorable expansion ratio.

The compact combustion volume of the AVL diesel coupled with the high swirl rates produced by the shrouded valves provide an ideal environment for combustion. The real question at hand is how does one go about improving the efficiency of the RCE while taking advantage of its high power to weight ratio. The controlled and high rates of pressure rise associated with the diesel engine during combustion are clearly a result of the ability to tailor the fuel injection schedule to a prescribed pattern. Thus, for the direct injected diesel engine the heat release schedule is determined by the structural constraints of the engine. In homogeneously charged spark ignition engines, the heat release schedule and A/F ratio for a given operating point are determined by the vagaries of combustion in a lean, turbulent mixture rather than by a fuel injection schedule.

Danieli (15) claims that the biggest loss in the RCE relative to the ideal fuel-air cycle is due to the finite combustion speed. Work by Cichanowitz and Sawyer (16) showed a slight improvement in indicated thermal efficiency when operating a rotary engine with hydrogen addition of up to 20 percent by mass to improve flame speed at low power levels. This effect should be studied at higher power levels 100 HP (75 kw) where "quenching effects" may not be as significant. Late burning means high heat transfer rates through the expansion stroke, as well as an effective expansion ratio that is less than a constant volume heat addition expansion ratio. It is thus important to determine how the fuel can be burned earlier in the expansion stroke.

Heat rejection to the coolant in the rotary tested, expressed as a percentage of input energy, was about 18 percent with an additional 7 percent rejected via the oil cooler for a total of 25 percent. This com-

8. Berkowitz, M., Jones, C. and Myers, D.: "Study of Advanced Rotary Combustion Engines for Commuter Aircraft," NASA CR-165399, July 1981.

9. Bujold, M. P.: "Small Car Transmission Test - Chevrolet Luv Transmission," NASA CR-159882, June 1980.

10. Rice, W. J. and Birchenough, A. G.: "Modular Instrumentation System for Real-Time Measurements and Control on Reciprocating Engines," NASA Technical Paper 1757, November 1980.

11. Schock, H. J., Rice, W. J. and Meng, P. R.: "Experimental Analysis of IMEP in a Rotary Combustion Engine," Paper 810150 presented at the SAE Automotive Engineering Congress, Cobo Hall, Detroit, February 1981.

12. Spindt, R. S.: "Air Fuel Ratios From Exhaust Gas Analysis," SAE Paper No. 650507, May 1965.

13. Burley, H. A., Meloeny, M. R. and Stark, T. L.: "Sources of Hydrocarbon Emissions in Rotary Engines," Paper 780419 presented at the SAE Automotive Engineering Congress, Cobo Hall, Detroit, February 1978.

14. Yamamoto, K. and Muroki, T.: "Development on Exhaust Emissions and Fuel Economy of the Rotary Engine at Toyo Kogo," Paper 780417 presented at the SAE Automotive Engineering Congress, Cobo Hall, Detroit, February 1978.

15. Danieli, G. A., Keck, J. C. and Heywood, J. B.: "Experimental and Theoretical Analysis of Wankel Engine Performance," Paper 780416, presented at the SAE Automotive Engineering Congress, Cobo Hall, Detroit, February 1978.

16. Cichanowicz, J. E. and Sawyer, R. F.: "Rotary Engine Combustion With Hydrogen Addition," SAE West Coast Meeting, Paper No. 760611, San Francisco, August 1976.